Spatiotemporal Pattern of Neuronal Injury Induced by DFP1 in Rats: A Model for Delayed Neuronal Cell Death Following Acute OP Intoxication

Yonggang Li[a,*], **Pamela J. Lein**[b,*], **Cuimei Liu**[a], **Donald A. Bruun**[b], **Teclemichael Tewolde**[a], **Gregory Ford**[a,c], and **Byron D. Ford**[a,†]

[a]Department of Neurobiology, Neuroscience Institute, Morehouse School of Medicine, Atlanta, GA, 30310, USA

[b]Department of Molecular Biosciences, School of Veterinary Medicine, University of California, Davis, CA, 95616, USA

[c]Department of Biology, Morehouse College, Atlanta, GA, 30310, USA

Abstract

Organophosphate (OP) neurotoxins cause acute cholinergic toxicity and seizures resulting in delayed brain damage and persistent neurological symptoms. Testing novel strategies for protecting against delayed effects of acute OP intoxication has been hampered by the lack of appropriate animal models. In this study, we characterize the spatiotemporal pattern of cellular injury after acute intoxication with the OP diisopropylfluorophosphate (DFP). Adult male Sprague Dawley rats received pyridostigmine (0.1 mg/kg, im) and atropine methylnitrate (20 mg/kg, im) prior to DFP (9 mg/kg, ip) administration. All DFP-treated animals exhibited moderate to severe seizures within minutes after DFP injection but survived up to 72 h. AChE activity was significantly depressed in the cortex, hippocampus, subcortical brain tissue and cerebellum at 1 h post-DFP injection and this inhibition persisted for up to 72 h. Analysis of neuronal injury by FluoroJade-B (FJB) labeling revealed delayed neuronal cell death in the hippocampus, cortex, amygdala and thalamus, but not the cerebellum, starting at 4 h and persisting until 72 h after DFP treatment, although temporal profiles varied between brain regions. At 24 h post-DFP injection, the pattern of FJB labeling corresponded to TUNEL staining in most brain regions, and FJB-positive cells displayed reduced NeuN immunoreactivity but were not immunopositive for astrocytic (GFAP), oligodendroglial (O4) or macrophage/microglial (ED1) markers, demonstrating that DFP causes a region-specific delayed neuronal injury mediated in part by apoptosis. These findings indicate the feasibility of this model for testing neuroprotective strategies, and provide insight regarding therapeutic windows for effective pharmacological intervention following acute OP intoxication.

[†]Corresponding author: Byron D. Ford Department of Neurobiology Neuroscience Institute Morehouse School of Medicine 720 Westview Drive, SW Atlanta, GA 30310 Phone: 1-404-756-5222 Fax: 1-404-348-1094 bford@msm.edu.
[*]These authors contributed equally to this work

CONFLICT OF INTEREST STATEMENT The authors declare no actual or potential conflicts of interest.

Keywords

INTRODUCTION

The September 11, 2001 attacks have increased awareness of terrorist threats, and the organophosphate (OP) neurotoxins figure prominently amongst chemicals considered credible threat agents. OP nerve agents are the most toxic of the chemical warfare agents and they have been used by terrorists in military combat and against civilian populations (Watson *et al.*, 1992; Jett, 2007). The less toxic, but more readily accessible OP pesticides cause a significant number of intoxications and several hundred thousand fatalities annually (Gunnell and Eddleston, 2003). Both OP nerve agents and OP pesticides cause acute toxicity by inhibiting acetylcholinesterase (AChE), the enzyme that hydrolyzes the neurotransmitter acetylcholine in the central and peripheral nervous systems. The consequent accumulation of acetylcholine at muscarinic and nicotinic receptors results in an acute cholinergic syndrome characterized by autonomic dysfunction, involuntary movements, muscle fasciculations, respiratory distress and seizures including status epilepticus (McDonough and Shih, 1997; Kwong, 2002; Leikin *et al.*, 2002).

OP toxicity is not limited to the acute toxicity phase and lingering debilitating neurological effects have been reported in individuals that survive the acute cholinergic crisis (Lemercier *et al.*, 1983; Savage *et al.*, 1988; Rosenstock *et al.*, 1991; Steenland *et al.*, 1994; Wesseling *et al.*, 2002; Hoffman *et al.*, 2007). Consistent with these clinical and epidemiological observations, experimental animal models of acute OP nerve agent intoxication demonstrate brain injury consequent to early convulsive seizures (McLeod, 1985; McDonough *et al.*, 1995; Shih *et al.*, 2003). In animals exposed to soman or VX, numerous injured neurons are observed in the lateral septum, cortex, thalamus, hippocampus and the amygdala one or more days following exposure (McDonough *et al.*, 1987; Petras, 1994; Baille *et al.*, 2001; Collombet *et al.*, 2006a).

Current post-exposure medical countermeasures against nerve agents (atropine, oximes, reversible AChE inhibitors and benzodiazepines) are useful in preventing mortality but are not sufficiently effective in protecting against chronic neurological disorders (McDonough and Shih, 1997; Kwong, 2002; Leikin *et al.*, 2002). Thus, there is a pressing need to establish animal models that replicate the early convulsive seizures yet have a relatively high survival rate to enable mechanistic studies and testing of novel therapeutic strategies for protecting against the delayed neurological sequelae associated with acute OP intoxication. The prototypical OP compound diisopropylfluorophosphate (DFP) has been used to model seizures and convulsions with subsequent behavioral deficits in rodents (Kim *et al.*, 1999; Auta *et al.*, 2004; Deshpande *et al.*, 2010; Wright *et al.*, 2010). DFP rapidly inhibits AChE, produces seizures and status epilepticus as determined by electroencephalography (Kim *et al.*, 1999; Deshpande *et al.*, 2010) and causes a high rate of mortality if animals are not treated aggressively to eliminate peripheral symptoms of cholinergic toxicity (Kim *et al.*, 1999). In animals pretreated with atropine, acute DFP intoxication has been shown to cause delayed apoptotic cell death in the CNS 24 and 48 h after DFP exposure as detected using TUNEL labeling (Kim *et al.*, 1999; Kadriu *et al.*, 2009). However, the spatiotemporal pattern of cell injury and the cell types injured following acute DFP intoxication remains poorly understood. In this study, we used FluoroJade-B (FJB) staining coupled with immunohistochemical localization of neuronal and glial cell markers to investigate the pattern of cellular injury in the rat brain at varying times after DFP exposure. The results demonstrate a region-specific, delayed neuronal cell injury following acute DFP

intoxication, and establish this as a useful model for testing novel therapeutic strategies for minimizing delayed brain damage following terrorist or suicidal uses of OP neurotoxins.

MATERIAL AND METHODS

Animals and DFP exposures

All animals used in these studies were treated humanely and with regard for alleviation of suffering and pain and all protocols involving animals were approved by the Animal Care and Use Committees of Morehouse School of Medicine, Oregon Health & Science University and University of California at Davis prior to the initiation of experimentation. Adult male Sprague-Dawley rats (280–320g; Charles River Laboratories, Hollister, CA) were housed individually in standard plastic cages in a temperature controlled room (22±2°C) on a 12 h reverse light-dark cycle. Food and water were provided *ad libitum*.

For DFP exposures, animals were anesthetized with 2% isoflurane (30% oxygen, 70% nitrous oxide) then injected im with pyridostigmine bromide (P1339, TCI America, Portland, OR) at 0.1 mg/kg in saline; and then 20 min later with atropine methylnitrate A0755, TCI America) at 20 mg/kg in saline. These drugs are centrally inactive (Shih *et al*., 1991) but effectively block peripheral OP neurotoxicity, thereby reducing mortality and facilitating detection of seizure symptoms (Kim *et al*., 1999). Ten minutes after the atropine injection, rats were injected ip with DFP (D0879, Sigma Chemical Co., St. Louis, MO) at 9 mg/kg diluted in sterile distilled water. DFP was always prepared fresh within 5 min before administration. Vehicle control rats received pyridostigmine and atropine and an equal volume (300 μl) of vehicle in place of DFP. Anesthesia was stopped immediately following injection of DFP or vehicle. The treatment groups included normal rats not injected with anything (n=4), vehicle control rats (n=4), and rats injected with DFP and then euthanized 1 h (n=4), 4 h (n=4), 8 h (n=6), 16 h (n=6), 24 h (n=6) or 72h (n=6) post-injection.

Behavioral scoring of seizure activity

Animals were continuously monitored for 5 h post-DFP injection and seizure behavior scored using a modified Racine's scale as previously described (Luttjohann *et al*., 2009). This scale was developed to describe pentylenetetrazole (PTZ)-induced seizures, as opposed to the amygdala-kindling model on which the Racine scale is based. This modified scale uses six different seizure intensity categories which reflect different onset latencies, patterns of occurrence and EEG patterns during high or low doses of PTZ. DFP-treated animals were scored with respect to the percent of animals exhibiting a specific behavior and the time to onset of each behavior.

Acetylcholinesterase (AChE) activity

Blood was collected in heparinized tubes by cardiac puncture immediately after euthanasia which was immediately followed by harvesting of brains with rapid dissection of brain regions on ice. All samples were snap frozen on dry ice and stored at −80°C. AChE activity was determined using the standard Ellman assay (Ellman *et al*., 1961) with 5,5'-dithio-bis(2-nitrobenzoic acid) (DTNB, Sigma) and acetylthiocholine iodide (ASChI, Sigma) as substrate. On the day of analysis, samples were thawed on ice and brain samples were homogenized in lysis buffer (0.1 M phosphate, pH 8.0 containing 0.1% Triton) using a Dounce homogenizer, centrifuged at $13,400 \times g$, and the supernatant collected for analysis. Assays were run against blanks containing DTNB. The reaction was started with the addition of ASChI after equilibration for 2–3 min. Hydrolysis of ASChI was determined by monitoring the change in absorbance at 405 nm. To inhibit pseudocholinesterase activity, 100 μM tetraisopropyl pyrophosphoramide was included in the assay. Data from brain samples were normalized using protein concentration as determined using the BCA assay

according to the manufacturer's directions (Pierce, Rockford, IL). AChE activity in blood samples was normalized according to blood volume after correcting for addition of heparin.

Histochemistry and immunohistochemistry

At the end of the DFP exposure period, most rats were deeply anesthetized with 2% isoflurane and perfused transcardially with saline followed by cold 4% paraformaldehyde solution in phosphate-buffered saline (PBS; pH 7.4) for 30 min. Brains were quickly removed and cryoprotected in 30% sucrose. A subset of rats whose brains were used for TUNEL labeling or O4 immunostaining were perfused with saline only prior to harvest and then snap frozen in dry ice. Coronal sections of 20 μm (for FJB labeling) or 10 μm (for double labeling studies) thickness were cryosectioned from the entire brain of each animal. Sections were mounted on slides which were stored at −80°C until use.

FJB (AG310, Millipore, Billerica, MA) labeling was performed according to the manufacturer's protocol with minor modifications. Briefly, after 30 min drying at 50°C, sections were postfixed with 4% paraformaldehyde for 15 min, washed with distilled water and then directly incubated in 0.06% potassium permanganate (KMnO$_4$) for 10 min on a shaker table followed by distilled water for 2 min. Sections were then incubated in a freshly prepared solution of 0.0004% FJB for 20 min, rinsed in distilled water and then dried at 50°C. Dried slides were cleared by immersion in xylene for 2 min before cover slipping with DPX mounting medium.

TUNEL labeling was performed using the *in situ* death detection kit from Roche Molecular Biochemicals (Indianapolis, IN). Briefly, fresh frozen brain sections were dried at room temperature for 30 min, postfixed with cold 4% paraformaldehyde for 15 min and then washed with PBS. Sections were incubated in 20 μg/ml Proteinase K solution for 10 min at room temperature to increase permeability. After 2 washes in PBS, sections were immersed in the TUNEL reaction mixture, containing biotinylated dUTP and terminal deoxynucleotidyl transferase (TdT) conjugated with the fluorochrome tetramethyl-rhodamine red for 60 min at 37°C in a dark, humidified atmosphere. The process was terminated by washing sections twice in a blocking buffer (PBS, 0.1% Triton X-100, and 5 mg/ml BSA). In each assay, negative controls were included using the same incubation procedure but omitting TdT in the process, whereas positive controls were performed by incubating the permeated sections with DNase (1 μg/ml) to induce DNA strand breakage.

For immunohistochemical studies, sections were dried at room temperature for 30 min. After rinsing with 0.01 M PBS, sections were blocked in PBS containing 5% normal goat serum and 0.3% triton-x100 for 1h at 4°C and then incubated for 1h at 37°C with primary antibodies of monoclonal mouse anti-NeuN (1:200, MAB314, Millipore), ED1(1:500, MAB1435, Millipore) or Cy3 conjugated anti-GFAP (1:500, C9205, Sigma). Sections labeled with anti-NeuN and ED1 antibodies were washed with PBS and incubated with a Cy3-conjugated goat anti-mouse IgG antibody (1:400, 115–165–166, Jackson ImmunoResearch Laboratory, West Grove, PA) for 1 h at room temperature. For 04 staining, fresh frozen brain sections were postfixed with 4% paraformaldehyde, blocked with 5% donkey serum in PBS and then incubated with the O4 primary IgM antibody (1:100, MAB345, Millipore) for 1h at 37°C. After washing with PBS, sections were incubated with Cy3- conjugated donkey anti-mouse antibody IgM (1:400, 715–165–140, Jackson Labs). Negative controls in which sections were reacted with secondary but not primary antibodies were run with each experiment.

For dual labeling studies, sections were first processed for either TUNEL labeling or immunohistochemistry as described above, and then processed using a modified method for FJB labeling. The modified protocol included brief immersion in 0.015% KMnO$_4$ for 1 min

followed by incubation in 0.0001% solution of FJB solution for 8 min. These modifications reduced the loss of immunohistochemical staining and minimized fluorescent bleed-through of FJB labeling during microscopy. The sections were rinsed with distilled water and cover slipped with mounting medium containing 0.1% acetic acid and 80% glycerin. Fluorescence was visualized via indirect fluorescence microscopy.

Quantification of FJB-positive cells

To quantify FJB labeling, every fifth section obtained from coronal sectioning of the entire brain of each rat was labeled with FJB. A Zeiss microscope equipped with CCD camera (Carl Zeiss Microimaging Inc, Thornwood, NY) was used to capture digital images of 5 sections at the same level across rats (as determined using a brain atlas) at 200× magnification. The number of FJB-positive cells was determined using Image Pro Plus software (Media Cybernetics, Inc., Bethesda, MD); only profiles of neuronal somas were counted and FJB-positive fragments were excluded. A mean value of FJB-positive cells per unit area within each brain region was obtained for each individual rat. These mean values from each individual rat were used as the statistical unit of measure for analysis by one-way ANOVA to determine statistically significant treatment effects.

RESULTS

Acute DFP neurotoxicity

Early studies (Kim *et al*., 1999) had reported that ip injection with DFP at 9 mg/kg following pretreatment with atropine methyl nitrate and pyridostigmine caused severe seizures in the absence of significant mortality in adult male Sprague Dawley rats. To examine the effects of OP-induced seizures on delayed neuronal cell injury, we replicated this model and used a modified Racine's scale (Luttjohann *et al*., 2009) to score the severity of seizures during a 5 h post-injection period (Figure 1). Behavioral changes were noted within minutes after DFP administration (Figure 1A) and escalated rapidly from facial jerking in more than 90% of animals to tonic-clonic seizures and/or wild jumping in approximately 50% of animals (Figure 1B). While all animals exhibited fairly severe seizure symptoms within minutes following DFP administration, the temporal profile of seizure activity over the 5 h post-injection observation period varied significantly between animals, with some animals exhibiting stage 5 or stage 6 behavior during the first 30–60 minutes after DFP injection and then lapsing into behavioral arrest with episodic facial jerking during the remainder of the observation period while other animals exhibited episodic stage 5 or stage 6 seizure activity throughout the 5 h post-injection period (Figure 1C). Less than 10% of the animals died within 24 h after DFP exposure using this atropine/pyridostigmine pretreatment paradigm.

Delayed neuronal injury associated with acute DFP intoxication

Animals were euthanized from 1 to 72 h following DFP injection and blood and brains collected immediately for quantification of acetylcholinesterase (AChE) activity and histological analyses of markers of brain injury. DFP treatment significantly depressed AChE activity in the blood and in all brain regions (Figure 2). AChE inhibition was more pronounced in the brain relative to the blood with the cortex, hippocampus, subcortical regions (striatum, thalamus and midbrain) and cerebellum all exhibiting > 90% inhibition at 1 hr after DFP administration relative to vehicle controls. AChE activity began to recover in all brain regions and in the blood with time; however, in all brain regions it was still significantly inhibited relative to vehicle controls at 72 h post-DFP injection.

To assess neuronal cell injury, brain sections from animals injected with DFP or vehicle were labeled with Fluoro-Jade B (FJB). Across all brain regions examined, there was

negligible FJB labeling in brain sections obtained from vehicle controls (Figures 3A, E, I, M, Q) or from DFP-treated rats 1 h after exposure (data not shown). In contrast, at later times after DFP treatment, FJB-positive cells were observed, although the temporal profile of FJB labeling varied between brain regions (Figure 3). As illustrated in representative images of hippocampal sections, FJB labeling was not detected in the hippocampal CA1 region until 8 h after DFP exposure (Figures 3B, C) and peaked at 24 hours (Figure 3G). However, FJB-positive cells were seen in the dentate gyrus at 4 h post-DFP injection (Figure 3F), with increasing numbers evident at 8 h (Figure 3G) and 24 h (Figure 3H) after DFP treatment. In the amygdala, relatively large numbers of FJB-positive cells were detected at 4 h after DFP exposure (Figure 3J) with significantly increased numbers of FJB-positive cells evident at 8 h (Figure 3K) and 24 h (Figure 3L) post-DFP injection. Other areas, such as the thalamus (Figures 3N, O, P) and cerebral cortex (Figures 3R, S, T) displayed FJB labeling that was slow to manifest but persisted at 24 h post DFP injection. The FJB positive cells were detected primarily in the superficial layers of the cingulate, retrosplenial, motor, somatosensory, visual and auditory cortices. FJB labeled cells were evenly distributed in the insular, perirhinal, ectohinal, piriform and entorhinal cortical layers. Despite significant AChE inhibition in the cerebellum, no FJB-positive cells were detected in this brain region up to 72 h post-DFP exposure (data not shown). As illustrated in a representative photomicrograph from the hippocampal dentate gyrus (Figure 4), counterstaining of sections from all brain regions with the nuclear label DAPI indicated that FJB-positive cells represent a subpopulation of neurons in each region.

Quantitative analysis of FJB labeling demonstrated that FJB-positive cells persisted for 72 h in all five brain regions in which DFP-induced cell injury was observed, although the temporal profile of cellular injury varied between brain regions (Figure 5). The amygdala and the dentate gyrus exhibited significant FJB labeling as early as 4 h post-DFP administration. In the amygdala, FJB labeling increased rapidly by 8 h and remained elevated out to 72 h after DFP injection. In the dentate gyrus, FJB labeling similarly increased by 8 h and remained elevated at 24 h but then decreased by 72 h following DFP administration. At the posterior outer blade of the dentate gyrus, 4 of 6 rats showed densely distributed FJB positive cells 72 h following DFP exposure while FJB-positive cells were not detected at earlier time points (data not shown). The cortex exhibited significant FJB labeling by 8 h which stayed elevated until 24 h and then declined by 72 h after DFP administration. The thalamus and hippocampal CA1 region did not exhibit significant FJB labeling until 16 h post-DFP injection. In the thalamus, FJB labeling reached a plateau at 16 h which persisted until 72 h; whereas in the CA1, the number of FJB-positive cells continued to increase at 24 h and began to decline by 72 h. The brain region that exhibited the greatest number of FJB-positive cells death was the amygdala (Figure 5), and as mentioned earlier, no FJB labeling was observed in the cerebellum at any of the time points examined (data not shown). We did not observe a specific relationship between the seizures and FJB labeling.

Apoptotic mechanisms contribute to DFP-induced neuronal cell injury

To determine whether apoptotic mechanisms contribute to the delayed cell injury caused by DFP, brain sections were double-labeled with FJB and TUNEL. TUNEL labeling was observed in all brain sections in which FJB labeling was present, but the relationship between the markers varied between brain regions. In the cerebral cortex, FJB labeling colocalized with TUNEL labeling in nearly all cells (Figures 6A, B, C). In contrast, in the CA1 region of the hippocampus there was a subpopulation of FJB-positive cells that did not co-localize with TUNEL labeling (Figures 6D, E, F). In substantia nigra, most TUNEL positive cells did not co-localize with FJB labeling (data not shown).

DFP primarily injures neuronal cells

To determine the identity of the FJB-positive cells in brain sections from DFP-exposed rats, FJB labeling was combined with immunohistochemical localization of the neuronal cell marker, NeuN (Mullen *et al*., 1992). As illustrated in representative photomicrographs from the cingulate cortex (Figure 7), large numbers of cells with high levels of NeuN immunoreactivity are observed in uninjured brain regions with negligible FJB labeling. However, in the area of injury as identified by the large number of FJB-positive cells, NeuN immunoreactivity is dramatically reduced (Figure 7, arrows). Similar results were observed in other cortical regions, the CA1 and dentate gyrus regions of the hippocampus, the thalamus and the amygdala (data not shown).

To confirm that FJB-positive cells were primarily neuronal, FJB labeling was combined with immunohistochemical localization of GFAP, a marker of astrocytes (Eng and Ghirnikar, 1994), O4, a marker of oligodendrocytes (Sommer and Schachner, 1981), ED1, a marker of macrophages and activated microglia (Dijkstra *et al*., 1985) and CD11b, a marker of macrophages and microglia (Mazzone and Ricevuti, 1995) in brain sections collected 24 h post-DFP injection. None of the FJB-positive cells were immunopositive for GFAP, as illustrated in the CA1 region of the hippocampus (Figure 8A), O4, as shown in the cingulate cortex (Figure 8B), ED1, as demonstrated in the dentate gyrus (Figure 8C) or CD11b, as shown in the somatosensory cortex (Figure 8D). The photomicrographs shown for these brain regions are representative of all the brain regions examined, which include other cortical regions, the CA1 and dentate gyrus regions of the hippocampus, the thalamus and the amygdala (data not shown).

DISCUSSION

Previous studies have demonstrated that acutely toxic doses of DFP cause significant seizure activity in the absence of mortality in rats pretreated with pyridostigmine and atropine (Kim *et al*., 1999; Deshpande *et al*., 2010), suggesting the potential of this model for investigating novel therapeutic strategies for minimizing brain damage following acute OP intoxication. Herein, we confirm that as determined using a modified Racine scale, this exposure paradigm triggers moderate to severe seizures within minutes after DFP administration. We also extend the characterization of this model by demonstrating significantly inhibited AChE activity in the blood and multiple brain regions evident as early as 1 h post-DFP treatment that persists in the brain for up to 72 h. Despite the rapid seizure activity and significant inhibition of AChE, the majority of DFP-treated animals (> 90%) survived throughout the 72 h observation period. These findings confirm the relevance of the model for testing novel medical countermeasures for minimizing delayed brain damage following acute OP intoxication.

Earlier reports of this DFP exposure model indicated increased levels of TUNEL labeling in several brain regions at 24 and 48 h following DFP administration (Kim *et al*., 1999; Kadriu *et al*., 2009). TUNEL labeling detects fragmented DNA during the late stages of apoptosis and is not restricted to any specific cell type (Gavrieli *et al*., 1992). In contrast, FluoroJade dyes, including FJB, label injured neurons regardless of mechanism of cell death (Schmued *et al*., 1997; Schmued and Hopkins, 2000a; Schmued and Hopkins, 2000b; Schmued *et al*., 2005), and thus provides a more comprehensive readout of neuronal cell damage. FJB has been used to detect and localize degenerating neurons and their processes in the brain tissue of animals subjected to neurotoxins (Schmued *et al*., 1997; Schmued, 2003; Schmued *et al*., 2005), traumatic brain injury (Lyeth *et al*., 2001; Sato *et al*., 2001; Hallam *et al*., 2004) and brain ischemia (Kokaia *et al*., 1998; Butler *et al*., 2002; Xu *et al*., 2004; Duckworth *et al*., 2005).

Acute DFP intoxication caused significant neuronal cell injury as indicated by a significant increase in FJB labeling. While peripheral signs of acute OP intoxication occurred within minutes of DFP administration, the FJB labeling was not observed until 4 h post-DFP injection. FJB labeling at 4 h was primarily limited to the dentate gyrus of hippocampus and the amygdala. It has been previously demonstrated that hippocampal brain regions are specifically vulnerable to a number of insults including excitotoxicity and ischemia that involve a delayed neuronal death (Schreiber and Baudry, 1995; Harry and Lefebvre d'Hellencourt, 2003). While the specific temporal pattern of FJB labeling varied between regions, it appeared in the CA1 region of the hippocampus, the cortex and the thalamus by 8 h, peaked between 8 and 24 h, and persisted in these five brain regions for up to 72 h following DFP administration. Interestingly, FJB labeling was not detected in the cerebellum at any of the time points examined, even though AChE was significantly depressed in this brain region. The reason for this marked difference between the cerebellum and the other brain regions examined is not known, but suggests that AChE inhibition per se is not sufficient to cause delayed neuronal cell death. Importantly, the spatial pattern of FJB labeling observed following acute DFP intoxication is strikingly similar to reports of animals exposed to OP nerve agents which demonstrate brain damage primarily in the hippocampus, amygdala, cortex and thalamus following seizures (McLeod, 1985; McDonough *et al*., 1995; Kim *et al*., 1999; Collombet *et al*., 2006a).

Several studies have reported that astrocytes and microglia can also be FJB positive under certain experimental conditions (Allen *et al*., 2000; Anderson *et al*., 2003; Damjanac *et al*., 2007). However, colocalization studies confirmed that across the five brain regions examined, FJB-positive cells were not immunoreactive for GFAP, O4, ED1 or CD11b, indicating that the FJB-positive cells were not astrocytes, oligodendrocytes, macrophages or microglia. NeuN is a neuronal specific nuclear protein in vertebrates and observed in most neuronal cell types throughout the nervous system except cerebellar Purkinje cells, olfactory bulb mitral cells, and retinal photoreceptor cells (Mullen *et al*., 1992). Following acute DFP intoxication, we observed that NeuN immunoreactivity was reduced or not detected in FJB positive cells in all injured brain regions. Loss of NeuN immunoreactivity has been reported in other models of neuronal injury, including trauma (Sato *et al*., 2001), ischemia (Unal-Cevik *et al*., 2004) and acute soman intoxication (Collombet *et al*., 2006b). In these previous reports, immunohistochemical and western blot analyses demonstrated that the loss of NeuN immunoreactivity was due to reduced NeuN antigenicity in degenerating neurons (Unal-Cevik *et al*., 2004; Collombet *et al*., 2006b). Thus, it seems reasonable that the decreased number of NeuN immunopositive cells in areas of injury in brain sections from DFP-treated animals and the reduced NeuN immunoreactivity associated with FJB-positive cells results from the loss of NeuN antigenicity in degenerating neurons. Collectively, our data indicate that the increased cellular injury observed in the brains of DFP-treated animals primarily reflects neuronal cell damage.

As an initial examination of the mechanisms associated with DFP-induced neuronal injury, we combined FJB staining with TUNEL labeling. Our results revealed that in most injured brain regions nearly all FJB labeling co-localized with TUNEL labeling. This is consistent with previous studies using the same DFP treatment paradigm that demonstrated apoptotic cells in the thalamus and amygdala 24 h after DFP administration (Kim *et al*., 1999). However, in this previous study, no notable TUNEL labeling was detected in the hippocampus. In our studies, we observed a subpopulation of FJB-positive cells that did not show co-localization with TUNEL in the CA1 region of the hippocampus. Collectively, these studies suggest that OP-induced brain injury in the hippocampus involves both necrotic and apoptotic forms of neuronal death. Our findings are consistent with ultrastructural studies demonstrating that the neuropathology produced by soman included both apoptosis and necrosis (Baille *et al*., 2005).

It is widely postulated that the behavioral deficits and persistent neurological symptoms observed following OP-induced cholinergic crisis and seizures (Lemercier *et al*., 1983; Savage *et al*., 1988; Rosenstock *et al*., 1991; Steenland *et al*., 1994; Wesseling *et al*., 2002; Hoffman *et al*., 2007) are the manifestation of the delayed neuronal death observed consequent to acute OP intoxication (Kim *et al*., 1999; Collombet *et al*., 2006a; Collombet *et al*., 2007). This has prompted significant research efforts to develop novel strategies for minimizing delayed neuronal damage. Our findings demonstrate that the rat model of acute DFP intoxication induces region-specific delayed neuronal death consequent to seizure. The pattern of neuronal injury closely mirrors the brain injury seen in rodent models following soman exposure, indicating the relevance of this model to exposures of concern in emergency planning and preparedness. While further research is required to determine the mechanisms that contribute to regional differences in the temporal pattern of neuronal cell injury following acute DFP intoxication, our data suggest that the model will be useful for pre-clinical trials of novel neuroprotectants, and further, identify endpoints to monitor for neuroprotective effectiveness and suggest a therapeutic window of 4 to 8 h post-exposure.

Acknowledgments

REFERENCES

Allen GV, Gerami D, Esser MJ. Conditioning effects of repetitive mild neurotrauma on motor function in an animal model of focal brain injury. Neuroscience. 2000; 99:93–105. [PubMed: 10924955]

Anderson KJ, Fugaccia I, Scheff SW. Fluoro-jade B stains quiescent and reactive astrocytes in the rodent spinal cord. J Neurotrauma. 2003; 20:1223–1231. [PubMed: 14651809]

Auta J, Costa E, Davis J, Guidotti A. Imidazenil: a potent and safe protective agent against diisopropyl fluorophosphate toxicity. Neuropharmacology. 2004; 46:397–403. [PubMed: 14975695]

Baille V, Clarke PG, Brochier G, Dorandeu F, Verna JM, Four E, Lallement G, Carpentier P. Soman-induced convulsions: the neuropathology revisited. Toxicology. 2005; 215:1–24. [PubMed: 16054742]

Baille V, Dorandeu F, Carpentier P, Bizot JC, Filliat P, Four E, Denis J, Lallement G. Acute exposure to a low or mild dose of soman: biochemical, behavioral and histopathological effects. Pharmacology, biochemistry, and behavior. 2001; 69:561–569.

Butler TL, Kassed CA, Sanberg PR, Willing AE, Pennypacker KR. Neurodegeneration in the rat hippocampus and striatum after middle cerebral artery occlusion. Brain Res. 2002; 929:252–260. [PubMed: 11864631]

Collombet JM, Carpentier P, Baille V, Four E, Bernabe D, Burckhart MF, Masqueliez C, Baubichon D, Lallement G. Neuronal regeneration partially compensates the delayed neuronal cell death observed in the hippocampal CA1 field of soman-poisoned mice. Neurotoxicology. 2006a; 27:201–209. [PubMed: 16309744]

Collombet JM, Four E, Fauquette W, Burckhart MF, Masqueliez C, Bernabe D, Baubichon D, Lallement G. Soman poisoning induces delayed astrogliotic scar and angiogenesis in damaged mouse brain areas. Neurotoxicology. 2007; 28:38–48. [PubMed: 16949671]

Collombet JM, Masqueliez C, Four E, Burckhart MF, Bernabe D, Baubichon D, Lallement G. Early reduction of NeuN antigenicity induced by soman poisoning in mice can be used to predict delayed neuronal degeneration in the hippocampus. Neurosci Lett. 2006b; 398:337–342. [PubMed: 16472911]

Damjanac M, Rioux Bilan A, Barrier L, Pontcharraud R, Anne C, Hugon J, Page G. Fluoro-Jade B staining as useful tool to identify activated microglia and astrocytes in a mouse transgenic model of Alzheimer's disease. Brain Res. 2007; 1128:40–49. [PubMed: 17125750]

Deshpande LS, Carter DS, Blair RE, DeLorenzo RJ. Development of a prolonged calcium plateau in hippocampal neurons in rats surviving status epilepticus induced by the organophosphate diisopropylfluorophosphate. Toxicol Sci. 2010; 116:623–631. [PubMed: 20498005]

Dijkstra CD, Dopp EA, Joling P, Kraal G. The heterogeneity of mononuclear phagocytes in lymphoid organs: distinct macrophage subpopulations in the rat recognized by monoclonal antibodies ED1, ED2 and ED3. Immunology. 1985; 54:589–599. [PubMed: 3882559]

Duckworth EA, Butler TL, De Mesquita D, Collier SN, Collier L, Pennypacker KR. Temporary focal ischemia in the mouse: technical aspects and patterns of Fluoro-Jade evident neurodegeneration. Brain Res. 2005; 1042:29–36. [PubMed: 15823250]

Ellman GL, Courtney KD, Andres V, Featherstone RM. A new and rapid colorimetric determination of acetylcholinesterase activity. Biochem Pharmacol. 1961; 7:88–95. [PubMed: 13726518]

Eng LF, Ghirnikar RS. GFAP and astrogliosis. Brain Pathol. 1994; 4:229–237. [PubMed: 7952264]

Gavrieli Y, Sherman Y, Ben-Sasson SA. Identification of programmed cell death in situ via specific labeling of nuclear DNA fragmentation. J Cell Biol. 1992; 119:493–501. [PubMed: 1400587]

Gunnell D, Eddleston M. Suicide by intentional ingestion of pesticides: a continuing tragedy in developing countries. Int J Epidemiol. 2003; 32:902–909. [PubMed: 14681240]

Hallam TM, Floyd CL, Folkerts MM, Lee LL, Gong QZ, Lyeth BG, Muizelaar JP, Berman RF. Comparison of behavioral deficits and acute neuronal degeneration in rat lateral fluid percussion and weight-drop brain injury models. J Neurotrauma. 2004; 21:521–539. [PubMed: 15165361]

Harry GJ, Lefebvre d'Hellencourt C. Dentate gyrus: alterations that occur with hippocampal injury. Neurotoxicology. 2003; 24:343–356. [PubMed: 12782100]

Hoffman A, Eisenkraft A, Finkelstein A, Schein O, Rotman E, Dushnitsky T. A decade after the Tokyo sarin attack: a review of neurological follow-up of the victims. Mil Med. 2007; 172:607–610. [PubMed: 17615841]

Jett DA. Neurological aspects of chemical terrorism. Ann Neurol. 2007; 61:9–13. [PubMed: 17262854]

Kadriu B, Guidotti A, Costa E, Auta J. Imidazenil, a non-sedating anticonvulsant benzodiazepine, is more potent than diazepam in protecting against DFP-induced seizures and neuronal damage. Toxicology. 2009; 256:164–174. [PubMed: 19111886]

Kim YB, Hur GH, Shin S. Organophosphate-induced brain injuries: delayed apoptosis mediated by nitric oxide. Environ Toxicol Pharmacol. 1999; 7:147–152.

Kokaia Z, Andsberg G, Yan Q, Lindvall O. Rapid alterations of BDNF protein levels in the rat brain after focal ischemia: evidence for increased synthesis and anterograde axonal transport. Exp Neurol. 1998; 154:289–301. [PubMed: 9878168]

Kwong TC. Organophosphate pesticides: biochemistry and clinical toxicology. Ther Drug Monit. 2002; 24:144–149. [PubMed: 11805735]

Leikin JB, Thomas RG, Walter FG, Klein R, Meislin HW. A review of nerve agent exposure for the critical care physician. Crit Care Med. 2002; 30:2346–2354. [PubMed: 12394966]

Lemercier G, Carpentier P, Sentenac-Roumanou H, Morelis P. Histological and histochemical changes in the central nervous system of the rat poisoned by an irreversible anticholinesterase organophosphorus compound. Acta neuropathologica. 1983; 61:123–129. [PubMed: 6637396]

Luttjohann A, Fabene PF, van Luijtelaar G. A revised Racine's scale for PTZ-induced seizures in rats. Physiol Behav. 2009; 98:579–586. [PubMed: 19772866]

Lyeth BG, Gong QZ, Shields S, Muizelaar JP, Berman RF. Group I metabotropic glutamate antagonist reduces acute neuronal degeneration and behavioral deficits after traumatic brain injury in rats. Exp Neurol. 2001; 169:191–199. [PubMed: 11312571]

Mazzone A, Ricevuti G. Leukocyte CD11/CD18 integrins: biological and clinical relevance. Haematologica. 1995; 80:161–175. [PubMed: 7628754]

McDonough JH Jr. Dochterman LW, Smith CD, Shih TM. Protection against nerve agent-induced neuropathology, but not cardiac pathology, is associated with the anticonvulsant action of drug treatment. Neurotoxicology. 1995; 16:123–132. [PubMed: 7603632]

McDonough JH Jr. McLeod CG Jr. Nipwoda MT. Direct microinjection of soman or VX into the amygdala produces repetitive limbic convulsions and neuropathology. Brain Res. 1987; 435:123–137. [PubMed: 3427447]

McDonough JH Jr. Shih TM. Neuropharmacological mechanisms of nerve agent-induced seizure and neuropathology. Neurosci Biobehav Rev. 1997; 21:559–579. [PubMed: 9353792]

McLeod CG Jr. Pathology of nerve agents: perspectives on medical management. Fundam Appl Toxicol. 1985; 5:S10–16. [PubMed: 4092882]

Mullen RJ, Buck CR, Smith AM. NeuN, a neuronal specific nuclear protein in vertebrates. Development. 1992; 116:201–211. [PubMed: 1483388]

Petras JM. Neurology and neuropathology of Soman-induced brain injury: an overview. J Exp Anal Behav. 1994; 61:319–329. [PubMed: 8169578]

Rosenstock L, Keifer M, Daniell WE, McConnell R, Claypoole K. Chronic central nervous system effects of acute organophosphate pesticide intoxication. The Pesticide Health Effects Study Group. Lancet. 1991; 338:223–227. [PubMed: 1676786]

Sato M, Chang E, Igarashi T, Noble LJ. Neuronal injury and loss after traumatic brain injury: time course and regional variability. Brain Res. 2001; 917:45–54. [PubMed: 11602228]

Savage EP, Keefe TJ, Mounce LM, Heaton RK, Lewis JA, Burcar PJ. Chronic neurological sequelae of acute organophosphate pesticide poisoning. Arch Environ Health. 1988; 43:38–45. [PubMed: 3355242]

Schmued LC. Demonstration and localization of neuronal degeneration in the rat forebrain following a single exposure to MDMA. Brain Res. 2003; 974:127–133. [PubMed: 12742630]

Schmued LC, Albertson C, Slikker W Jr. Fluoro-Jade: a novel fluorochrome for the sensitive and reliable histochemical localization of neuronal degeneration. Brain Res. 1997; 751:37–46. [PubMed: 9098566]

Schmued LC, Hopkins KJ. Fluoro-Jade B: a high affinity fluorescent marker for the localization of neuronal degeneration. Brain Res. 2000a; 874:123–130. [PubMed: 10960596]

Schmued LC, Hopkins KJ. Fluoro-Jade: novel fluorochromes for detecting toxicant-induced neuronal degeneration. Toxicol Pathol. 2000b; 28:91–99. [PubMed: 10668994]

Schmued LC, Stowers CC, Scallet AC, Xu L. Fluoro-Jade C results in ultra high resolution and contrast labeling of degenerating neurons. Brain Res. 2005; 1035:24–31. [PubMed: 15713273]

Schreiber SS, Baudry M. Selective neuronal vulnerability in the hippocampus--a role for gene expression? Trends Neurosci. 1995; 18:446–451. [PubMed: 8545911]

Shih TM, Duniho SM, McDonough JH. Control of nerve agent-induced seizures is critical for neuroprotection and survival. Toxicol Appl Pharmacol. 2003; 188:69–80. [PubMed: 12691725]

Shih TM, Koviak TA, Capacio BR. Anticonvulsants for poisoning by the organophosphorus compound soman: pharmacological mechanisms. Neurosci Biobehav Rev. 1991; 15:349–362. [PubMed: 1683477]

Sommer I, Schachner M. Monoclonal antibodies (O1 to O4) to oligodendrocyte cell surfaces: an immunocytological study in the central nervous system. Dev Biol. 1981; 83:311–327. [PubMed: 6786942]

Steenland K, Jenkins B, Ames RG, O'Malley M, Chrislip D, Russo J. Chronic neurological sequelae to organophosphate pesticide poisoning. Am J Public Health. 1994; 84:731–736. [PubMed: 8179040]

Unal-Cevik I, Kilinc M, Gursoy-Ozdemir Y, Gurer G, Dalkara T. Loss of NeuN immunoreactivity after cerebral ischemia does not indicate neuronal cell loss: a cautionary note. Brain Res. 2004; 1015:169–174. [PubMed: 15223381]

Watson N, Barnes PJ, Maclagan J. Actions of methoctramine, a muscarinic M2 receptor antagonist, on muscarinic and nicotinic cholinoceptors in guinea-pig airways in vivo and in vitro. Br J Pharmacol. 1992; 105:107–112. [PubMed: 1596672]

Wesseling C, Keifer M, Ahlbom A, McConnell R, Moon JD, Rosenstock L, Hogstedt C. Long-term neurobehavioral effects of mild poisonings with organophosphate and n-methyl carbamate pesticides among banana workers. Int J Occup Environ Health. 2002; 8:27–34. [PubMed: 11843437]

Wright LK, Liu J, Nallapaneni A, Pope CN. Behavioral sequelae following acute diisopropylfluorophosphate intoxication in rats: comparative effects of atropine and cannabinomimetics. Neurotoxicol Teratol. 2010; 32:329–335. [PubMed: 20034559]

Xu Z, Jiang J, Ford G, Ford BD. Neuregulin-1 is neuroprotective and attenuates inflammatory responses induced by ischemic stroke. Biochem Biophys Res Commun. 2004; 322:440–446. [PubMed: 15325249]
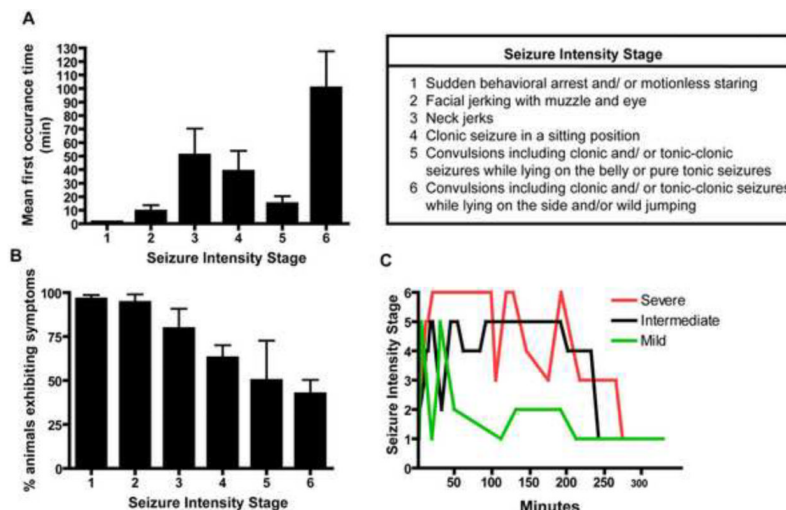
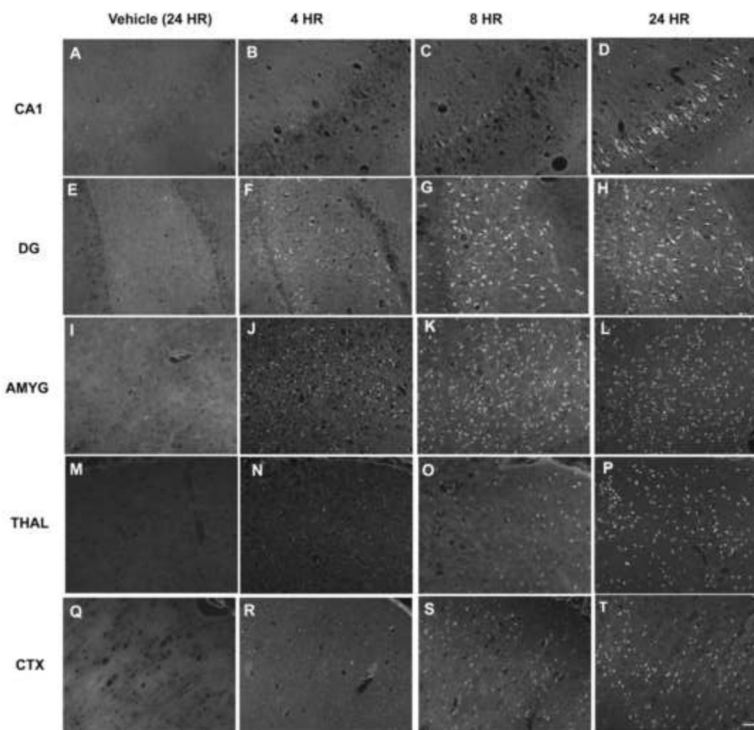**Figure 1. Seizure activity in rats following acute DFP intoxication**
Rats were pretreated with pyridostigmine (0.1 mg/kg, im) and atropine methyl nitrate (20 mg/kg, im) 30 or 10 min, respectively, prior to ip injection of DFP (9 mg/kg) or an equal volume (300 μl) of vehicle. Seizure behavior was monitored continuously for 5 h post-DFP injection and scored using a revised Racine's scale (Luttjohann *et al*., 2009) as described in the Table. Seizure behaviors were not observed in vehicle controls (data not shown). The seizure behaviors elicited by DFP in rats pretreated with pyridostigmine and atropine were variable within the treatment group (n=12) as evidenced by the mean onset time for each specific behavior following DFP injection (A) and the percentage of DFP-treated animals exhibiting any specific seizure behavior (B). (C) Representative activity profiles of rats exhibiting three different patterns of seizure behaviors following DFP injection. Data in panels A and B are expressed as $X \pm SE$ (n includes only those animals exhibiting the specific behavior).
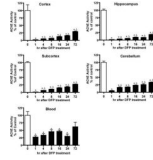
Figure 2. Time course of acetylcholinesterase (AChE) inhibition in specific rat brain regions following acute DFP intoxication
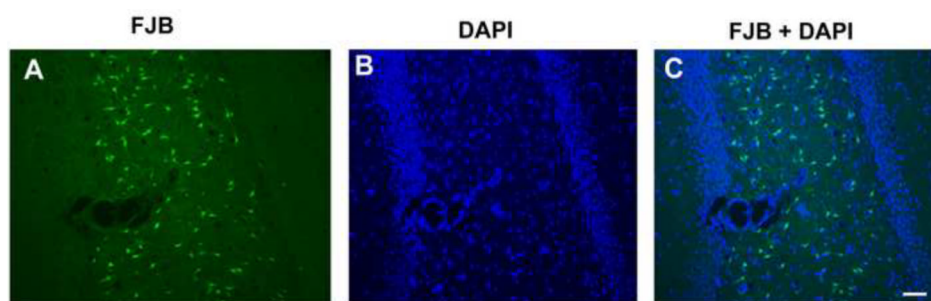
Anesthetized rats were pretreated with pyridostigmine (0.1 mg/kg, im) and atropine methyl nitrate (20 mg/kg, im) 30 or 10 min, respectively, prior to injection of DFP (9 mg/kg, ip) or an equal volume (300 μl) of vehicle (water). AChE activity was determined in whole blood and specific brain regions collected immediately after euthanasia at varying times after DFP injection and raw values converted to a percentage of the mean AChE activity in corresponding tissue from vehicle controls. Data are expressed as $X \pm SE$ (n = 5 per treatment group). Statistically significant differences were determined using one way ANOVA with *post hoc* Tukey's test; *$p<0.01$ compared to vehicle control; $^{\Delta}p<0.01$ compared to 1 h post-DFP injection.

Figure 3. Acute DFP intoxication elicits neuronal injury in the brain that is time and region dependent
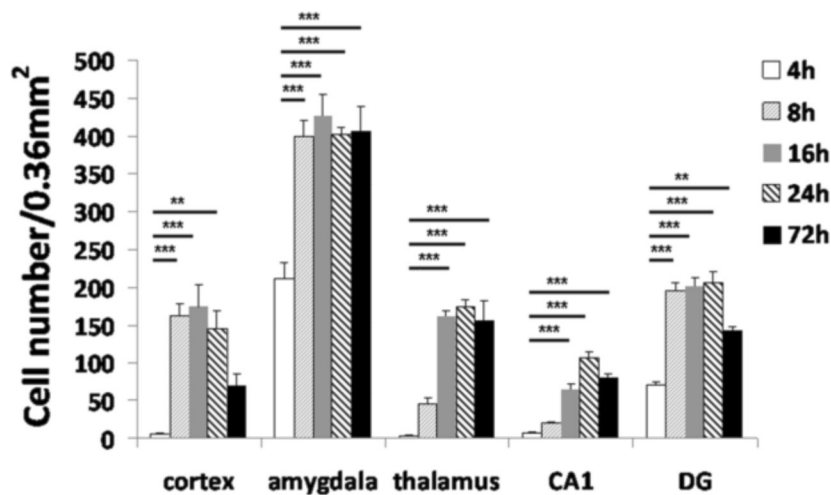
Anesthetized rats were pretreated with pyridostigmine (0.1 mg/kg, im) and atropine methyl nitrate (20 mg/kg, im) 30 or 10 min, respectively, prior to ip injection of DFP (9 mg/kg) or an equal volume of vehicle (CTRL, panels A, E, I, M and Q). DFP-treated animals were euthanized and their brains collected for staining with Fluoro-Jade B (FJB) at 4 h (B, F, J, N and R), 8 h (C, G, K, O and S) or 24 h (D, H, L, P and T) after DFP injection. Representative photomicrographs of FJB labeling in the CA1 region of the hippocampus (CA1; A–D), hippocampal dentate gyrus (DG; E–H), amygdala (AMYG; I–L), dorsal thalamus (THAL; M–P) and somatosensory cortex (CTX; Q–T) for each treatment group. Bar = 100 μm.

Figure 4. Acute DFP intoxication injures a subpopulation of neurons
Representative photomicrographs of (A) Fluoro-Jade B (FJB) labeling and (B) DAPI
staining in the hippocampal CA1 region of a rat 24 h post-DFP injection. All animals were
anesthetized and pretreated with pyridostigmine (0.1 mg/kg, im) and atropine methyl nitrate
(20 mg/kg, im) prior to DFP (9 mg/kg, ip) injection. (C) A merged image illustrates that
only a subpopulation of DAPI-positive cells is labeled with FJB. Bar = 100 μm.

Figure 5. Acute DFP intoxication elicits neuronal injury in the brain that is time and region dependent
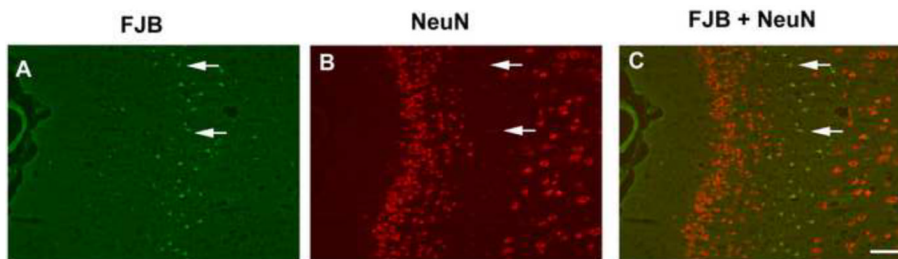
Anesthetized rats were pretreated with pyridostigmine (0.1 mg/kg, im) and atropine methyl nitrate (20 mg/kg, im) 30 or 10 min, respectively, prior to ip injection of DFP (9 mg/kg) or an equal volume (300 μl) of vehicle. DFP-treated rats were euthanized at varying times after DFP injection and the brains collected for staining with Fluoro-Jade B (FJB). The number of FJB-positive cells in specific brain regions at the same level as determined using a brain atlas was quantified from digital images of coronal sections (200× magnification). Control animals did not display FJB labeling (data not shown). Significant increases in FJB-positive cells were observed in multiple brain regions, although the magnitude and temporal profile varied between brain regions. Data are expressed as $X \pm SE$ (n=4 to 6 animals per treatment group). Statistically significant differences were identified using one way ANOVA with *post hoc* Tukey's test; **p<0.01 and ***p<0.001 compared to region-matched 4 h post-DFP injection samples.
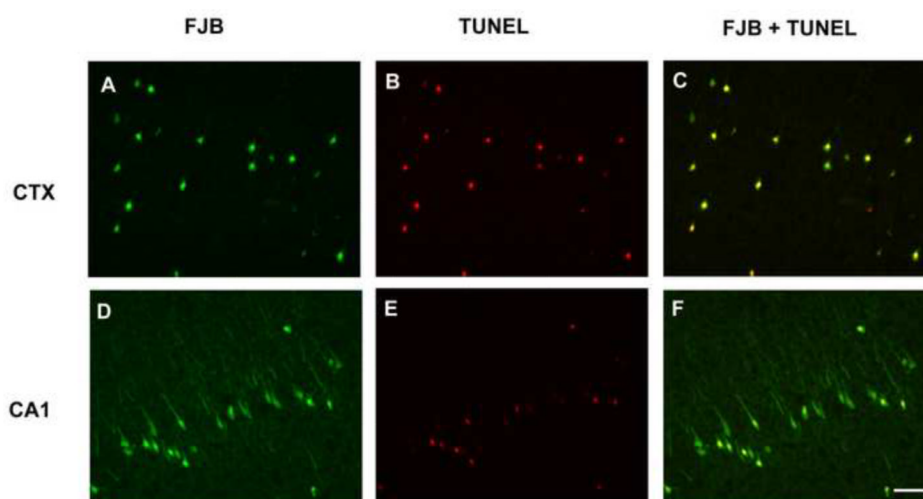
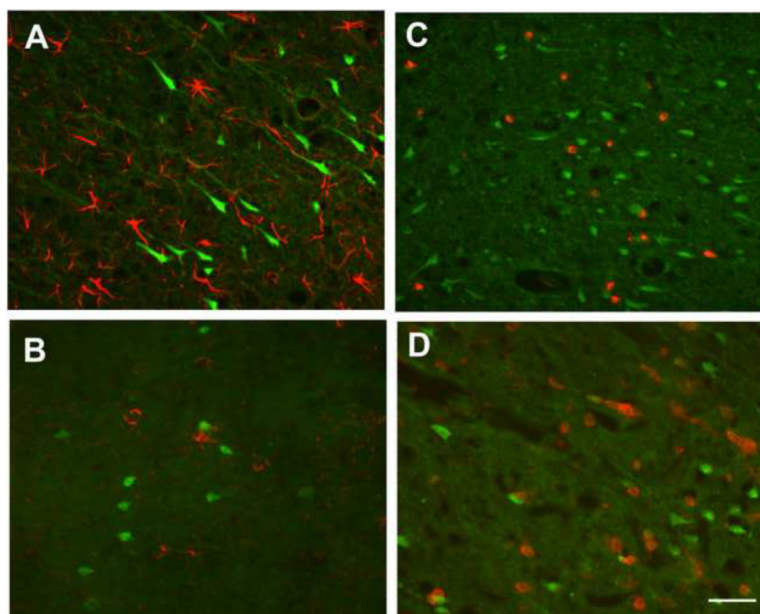**Figure 6. Co-localization of Fluoro-Jade B (FJB) labeling and TUNEL labeling at 24 h post-DFP injection**

Anesthetized rats were pretreated with pyridostigmine (0.1 mg/kg, im) and atropine methyl nitrate (20 mg/kg, im) 30 or 10 min, respectively, prior to ip injection of DFP (9 mg/kg). At 24 h post-DFP injection, rats were euthanized and brain sections co-labeled with FJB (green, A and D) and TUNEL (red, B and E). TUNEL labeling was examined in the amygdala, cortex, thalamus and hippocampus from three DFP-treated rats. Representative photomicrographs are shown from the cingulate cortex (CTX, panels A–C) and hippocampus CA1 (panels D–F). Merged images illustrates that most FJB-positive cells in the cingulate cortex also exhibit TUNEL labeling (C); whereas in the hippocampus CA1, a subset of cells exhibit co-labeling with FJB and TUNEL (F). Bar = 100 μm.

Figure 7. NeuN labeling is reduced in injured neurons at 24 h post-DFP injection
Anesthetized rats were pretreated with pyridostigmine (0.1 mg/kg, im) and atropine methyl nitrate (20 mg/kg, im) 30 or 10 min, respectively, prior to ip injection of DFP (9 mg/kg). At 24 h post-injection, rats were euthanized and brain sections labeled with Fluoro-Jade B (FJB, green, A) and immunostained for NeuN (red, B). NeuN immunoreactivity was examined in the amygdala, cortex, thalamus and hippocampus from three DFP-treated rats. Representative photomicrographs from the cingulate cortex show that in areas of neuronal injury as identified by FJB labeling (arrows in A), the relative intensity of NeuN (arrows in B) is dramatically reduced relative to large numbers of neurons with relatively high levels of NeuN immunoreactivity in uninjured brain regions (B). A merged image demonstrates FJB labeling in cells with low-NeuN expression (C; arrows). Bar = 100 μm.

Figure 8. Non-neuronal cells are not labeled by Fluoro-Jade B (FJB) in brains from rats acutely intoxicated with DFP

Anesthetized rats were pretreated with pyridostigmine (0.1 mg/kg, im) and atropine methyl nitrate (20 mg/kg, im) 30 or 10 min, respectively, prior to ip injection of DFP (9 mg/kg). Brain sections collected at 24 h post-injection were labeled with FJB and immunostained for the astrocyte-selective antigen GFAP (A), the oligodendrocytes antigen O4 (B), the activated macrophage antigen ED1 (C) or the microglia antigen CD11b (D). FJB labeling and immunoreactivity for these various markers were examined in the amygdala, cortex, thalamus and hippocampus from three DFP-treated rats. Representative images from the hippocampus CA1 (A), cingulate cortex (B), dentate gyrus (C) and somatosensory cortex (D) illustrate the general finding across all four brain regions that FJB-labeled cells do not co-localize with GFAP, O4, ED1 or CD11b-immunoreactivity. Bar = 100 μm.